Environ. Sci. Technol. **1998**, *32,* 3549−3555

A Distributed Reactivity Model for Sorption by Soils and Sediments. 11. Slow Concentration-Dependent Sorption Rates

WEILIN HUANG AND
WALTER J. WEBER, JR.*
Environmental and Water Resources Engineering, Department of Civil and Environmental Engineering, The University of Michigan, Ann Arbor, Michigan 48109-2125

Long-term temporal phase distribution relationships (PDRs) were measured for sorption of a hydrophobic organic contaminant probe by seven EPA reference soils and sediments and six shale and kerogen samples. The times required for attainment of apparent sorption equilibrium by the phenanthrene probe were found to be highly dependent upon the aqueous phase-solute concentration, $C(t)$, for a given sorbent, and the type of soil organic matter (SOM) associated with a particular sorbent. Organic-carbon-normalized single-point temporal distribution ratios corresponding to low residual solution phase concentrations were found to approach their respective apparent equilibrium values after times ranging from several days to 90 days for the EPA soils and sediments and from 90 days to $\geq$ 368 days for the shales and kerogens. Conversely, at residual solution phase concentrations 2 orders of magnitude larger, apparent equilibrium conditions were attained within a few hours for the EPA soils and sediments and within a year for the shale and kerogen samples. The observed dependencies of sorption rate on $C(t)$ and on the type of SOM appear to result from differences in solute diffusion behavior within chemically reduced and structurally condensed SOM domains and that in highly amorphous SOM domains. In the former case the very slow and concentration-dependent non-Fickian behavior observed is likely attributable to the slow and energetically driven reconfiguration of local condensed SOM structures to accommodate solute migration into the matrixes. The results of the study extend the applicability of the Dual Reactive Domain Model introduced earlier in this series of papers to the interpretation and description of sorption rate behavior.

Introduction

Rates of sorption of hydrophobic organic contaminants (HOCs) by natural solids (soils, sediments, aquifer, and aquitard materials) have been shown to be biphasic in character, generally involving a fast initial uptake followed by a very slow sustained approach to apparent equilibrium (e.g., refs *1*−*6*). The latter phenomenon can significantly impact the fate and transport of HOCs in subsurface systems as well as the effectiveness of contaminant remediation schemes for such systems (*7*, *8*). Although extensive research has been conducted on HOC sorption in general, there have been few quantitative investigations of slow sorption over extended time periods and of the effects of such gradual "aging" of sorption on subsequent desorption. Indeed, the phenomenon of slow sorption has been examined systematically and rigorously in only one previous study (*4*), and the associated mechanisms are currently not well understood (*8*).

The principal objective of the work described here was to examine rates of solute sorption over extended periods of time by various natural solids having markedly different physical and chemical properties and then to relate those rate behaviors to the sorbent properties. Potential rate controlling mechanisms were elucidated by comparing rate patterns exhibited by sorbents of different properties under different concentration conditions. Observed long-term sorption behaviors were then interpreted in the context of the dual reactive domain model (DRDM) described earlier in this series (*9*).

Previous studies have demonstrated that sorption by natural solids requires times ranging from days to months to attain apparent equilibrium. The term "apparent" is used here to describe a state in which no measurable changes in solute uptake are observed over extended periods of time. Ball and Roberts (*4*) found that sorption of perchloroethylene and tetrachlorobenzene by sandy materials takes 10−100 days to attain apparent equilibrium, and the fitting of an intraparticle diffusion model to their rate data suggested that much longer times would be required to attain true equilibrium. The results of several related slow sorption studies summarized by Pignatello (*10*) and Pignatello and Xing (*8*) suggest that times required for sorption by soils and sediments to attain apparent equilibrium may vary from days to years.

It has been proposed variously that such slow sorption phenomena can be attributed to retarded sorbate diffusion: (i) within soil organic matter (SOM) matrixes (*6*, *8*−*14*); (ii) in the meso- and micropore structures of inorganic matrixes (*4*, *5*, *8*, *15*−*19*); and, (iii) to and within SOM matrixes encapsulated by inorganic coatings within sorbent particles or aggregates (*20*). With respect to the first proposition, a number of investigators have drawn analogies between different types of SOM and different types of synthetic organic polymers, suggesting that sorption into rubbery ("soft") polymers is fast while that into glassy ("hard") organic polymers is slow (*6*, *8*−*14*). LeBoeuf and Weber (*9*) provided evidence to support this analogy; i.e., they demonstrated that soil organic matter, like synthetic organic polymers, manifests transitions from glassy states to rubbery states at elevated temperatures. The second proposition regarding slow diffusion has for the most part been based on the fitting of sorption rate data collected in column or batch systems to intraparticle diffusion models (e.g., refs *4*, *12*). This has been challenged by the results of several recent reports entailing experiments carefully designed to test the hypothesis (*16*, *17*, *21*). In the fifth paper of this series, for example, we have shown that rates of phenanthrene uptake by highly porous silica gels are rapid, largely because pore surfaces within meso- and micropore structures of pure inorganic solids are polar and preferentially sorb water molecules, forming structured vicinal water films (*21*). This results in low accessibility of pore surfaces to HOC molecules; i.e., no actual diffusion occurs within such pores. Reinhard and co-workers (*16*, *17*) did observe that some fractions of volatile chlorinated compounds (e.g., trichloroethylene) presorbed

* Corresponding author phone: (734)763-2274; fax: (734)763-2275; e-mail: wjwjr@engin.umich.edu.

10.1021/es970764n CCC: $15.00
Published on Web 10/02/1998

on mesoporous silicas under near-saturation conditions do desorb at slower rates and attributed this behavior to solute diffusion within micropores. However, they also found that such fractions represented only ~5% of the presorbed amounts of solute, thus effectively confirming the relatively minor contribution of mineral micropore sorption and diffusion. The third hypothesis regarding sorption into SOM encapsulated within inorganic coatings in soil particles could certainly, if true, produce a very protracted process involving diffusion both across inorganic envelops and within encapsulated SOMs (*20*).

This study was designed to test more exhaustively the hypothesis that sorption into condensed SOM matrixes is responsible for slow rates of uptake of HOCs by soils and sediments. Experimental investigations described in the first 10 papers in this DRM series (*6, 14, 21−28*) and in reports by Pignatello and co-workers (*29, 30*) have suggested that soil and sediment organic matter comprises two fundamentally different types of SOM. In the fourth paper of the series (*6*) we held that rates of sorption into condensed SOM matrixes are slow and likely limited by non-Fickian diffusion processes in which diffusion rate coefficients are functions of solid-phase and/or aqueous-phase sorbate concentrations. We here report the results of experiments in which the temporal sorptive phase distribution relationship (PDR) technique described in that earlier paper was employed to measure rates of sorption over periods ranging from a few days to as long as one year for 13 natural sorbents and the solute, phenanthrene, a three ring polynuclear aromatic hydrocarbon HOC probe. A Freundlich-like PDR equation incorporating time-dependent parameters was used to fit the measured sorption rate data.

Experimental Section

Sorbents and Their Characterization. The 13 natural sorbents included three shale samples (Norwood, Lachine, and Paxton), three kerogen samples obtained by demineralizing the three shales, and seven soil and sediment samples (EPA-8, -9, -13, -20, -22, -23, and -26) generously provided by Dr. W. L. Banwart of the Department of Agronomy at the University of Illinois at Champaign Urbana. These samples have been used in our previous studies of phenanthrene sorption and desorption under apparent equilibrium or rate-limited conditions, and their major physical and chemical properties have been detailed elsewhere (*6, 27, 28, 31*), as have alternative procedures for inferring the extent or relative quantity of condensed vs amorphous SOM in a soil or sediment (*9, 14, 22, 23*). The demineralization process applied to the shales has been described by Huang and Weber (*28*) and in the references listed therewith.

Sorbate and Background Solutions and Analytical Techniques. The procedures employed for preparation of background solutions (0.005 M $CaCl_2$) and initial solute solutions and analytical techniques are detailed elsewhere (*6, 27, 28, 31*).

Biological Activity Control. Sodium azide (NaN_3) was added to background solutions at a level of 100 mg/L to inhibit biological activity. Selective checks for bioactivity were conducted for the EPA-20, -22, -23 geosorbents after completion of 368-day sorption experiments. This was done by plating mixtures of supernatant and solids from two parallel reactors having the highest residual $C(t)$ values on a growth medium containing nutrients and phenanthrene as the sole substrate. The plates were inoculated at 32 °C for 2 days. No biological activity was observed, suggesting that no biodegradation of phenanthrene had occurred in any of the three systems checked.

Sorption Experiments. Sorption experiments were conducted at a temperature of 25 ± 0.3 °C using flame-sealed glass ampules (Kimble, 60 mL for shale and kerogen samples and 25 mL for the seven other samples) as completely mixed batch reactor (CMBR) systems. Preliminary tests were performed to determine a constant sorbent-to-solution ratio for each sorbent-solution system that would yield a 30−70% reduction in aqueous-phase solute concentration in each reactor at the completion of an experiment. The reactors run for ≤30 days were continuously tumbled from top to bottom at 13 rpm, whereas those run for >30 days were continuously tumbled during the first 30 days and then disturbed (i.e., tumbled) by hand twice a week. After mixing, the reactors were set upright for 2 days to allow suspended solids to settle. This method was employed because the ampules used would not withstand high centrifugation spin speeds. No measurable difference in sorption was found in preliminary tests using this settling method and two different centrifugation methods (at 2000 and 4500 rpm; glass centrifuge bottles as reactors). The observation time reported here for each PDR measurement includes times for both mixing and settling. Complete details of the experimental procedures employed for sorption and desorption measurements have been reported previously (*6, 27, 31*).

Control reactors containing no sorbent were run simultaneously for all experiments to evaluate solute loss to reactor components. The results revealed that aqueous phenanthrene solutions at initial concentrations of 58.2, 148.5, 394.8, 712.6, 912.5 μg/L changed to 54.9, 144.5, 396.8, 703.9, 902.1 μg/L, respectively, over a period of approximately one year (368 days). Losses were thus neglected in the mass balance calculations for solid-phase solute concentrations.

Results and Discussion

Data Reduction. Sorption data obtained at a given time, t, for a specific sample were fitted with a Freundlich-like temporal PDR equation having the form

$$q(t) = K_F(t)(C(t))^{n(t)} \quad (1)$$

or,

$$\log q(t) = \log K_F(t) + n(t) \log C(t) \quad (2)$$

The time dependent parameters $K_F(t)$ and $n(t)$ are the capacity parameter and linearity factor, respectively, and $q(t)$ and $C(t)$ are the solid-phase and aqueous-phase solute concentrations at a given t expressed in units of μg/g and μg/L, respectively. A linear regression procedure employing SYSTAT software (Version 5.2.1, SYSTAT, SYSTAT Inc., Pittsburgh) was utilized for fitting eq 2 to logarithmically transformed sorption data. Resulting values of $\log K_F(t)$ and $n(t)$, along with their respective 95% confidence levels, numbers of observations, and R^2 values, are given in Table 1. The short term (<14 days) PDR parameters presented in ref *6* for EPA-22 and -23 are also shown in Table 1 for convenience of comparison. Representative sorption data for one of the 13 samples, Lachine shale, are shown in Figure 1. Temporal PDR parameters ($K_F(t)$ and $n(t)$) for the Lachine shale sample are plotted against logarithmic time in Figure 2.

To assist in the interpretation of the experimental data with respect to rate of approach to apparent equilibrium, the fitted Freundlich parameters were employed to determine single-point values of $q(t)$ for arbitrary index values of residual/aqueous phase concentration, $C^*(t)$. The ratio of these single-point values, $q(t)/C^*(t)$, was then divided by the organic carbon fraction of a sample, f_{oc}, values of which are included in Table 1. As illustrated in eq 3, this calculation

TABLE 1. Parameters for Temporal Phase Distribution Relationships[a]

sorbent	t	log $K_F(t)$[b]	$n(t)$	$K^*_{oc}(t)$[c] $C^*(t) = 5\ \mu g/L$	$K^*_{oc}(t)$[c] $C^*(t) = 500\ \mu g/L$	R^2	N[d]
EPA-26 sediment	14 d	−0.036 (0.026)[e]	0.764 (0.016)[f]	42.5	14.3	0.999	16
$f_{oc} = 1.50 \times 10^{-2}$	42 d	−0.038 (0.065)	0.777 (0.032)	43.2	15.5	0.996	12
EPA-23 sediment	1 m	−0.979 (0.099)	0.926 (0.033)	3.9	2.8	0.998	12
$f_{oc} = 2.57 \times 10^{-2}$	5 m	−0.684 (0.128)	0.880 (0.044)	7.2	4.1	0.995	12
	10 m	−0.539 (0.080)	0.855 (0.028)	9.6	4.9	0.998	12
	30 m	−0.365 (0.074)	0.833 (0.027)	13.9	6.4	0.998	12
	60 m	−0.234 (0.084)	0.803 (0.031)	17.8	7.2	0.997	12
	120 m	−0.100 (0.055)	0.782 (0.020)	23.5	8.6	0.999	12
	240 m	−0.008 (0.034)	0.748 (0.013)	27.5	8.6	1.000	12
	720 m	0.057 (0.035)	0.754 (0.013)	32.2	10.4	1.000	12
	1 d	0.137 (0.047)	0.730 (0.018)	37.3	10.7	0.999	12
	2 d	0.176 (0.058)	0.722 (0.023)	40.3	11.2	0.999	12
	14 d	0.225 (0.079)	0.727 (0.017)	47.6	14.4	0.996	19
	30 d	0.288 (0.047)	0.680 (0.024)	48.7	11.2	0.996	16
	90 d	0.408 (0.014)	0.680 (0.007)	64.2	14.7	0.999	16
	182 d	0.390 (0.050)	0.676 (0.026)	61.2	13.8	0.996	16
	368 d	0.420 (0.052)	0.676 (0.027)	65.6	14.8	0.995	16
EPA-22 sediment	1 m	−1.181 (0.196)	1.059 (0.092)	4.3	5.7	0.986	12
$f_{oc} = 1.65 \times 10^{-2}$	5 m	−1.109 (0.213)	1.096 (0.101)	5.4	8.5	0.987	12
	10 m	−1.036 (0.154)	1.119 (0.0745)	6.7	11.6	0.992	12
	30 m	−0.553 (0.072)	1.016 (0.037)	17.2	18.5	0.998	12
	60 m	−0.340 (0.097)	0.936 (0.048)	24.7	18.4	0.995	12
	180 m	−0.245 (0.088)	0.919 (0.046)	29.9	20.6	0.995	12
	1 d	−0.233 (0.075)	0.876 (0.041)	28.7	16.2	0.996	12
	14 d	−0.205 (0.041)	0.888 (0.046)	31.2	18.6	0.991	20
	30 d	−0.049 (0.049)	0.820 (0.029)	40.0	17.5	0.996	16
	90 d	0.0623 (0.0283)	0.796 (0.027)	49.8	19.5	0.992	12
	182 d	0.1003 (0.0285)	0.776 (0.030)	52.6	18.8	0.995	14
	368 d	0.0436 (0.0205)	0.815 (0.029)	49.2	21.0	0.996	12
EPA-20 soil	14 d	−0.192 (0.030)	0.756 (0.014)	33.4	10.9	0.994	20
$f_{oc} = 1.18 \times 10^{-2}$	30 d	−0.202 (0.022)	0.722 (0.011)	30.8	8.6	0.999	16
	90 d	−0.055 (0.028)	0.701 (0.014)	41.9	10.6	0.994	16
	182 d	−0.120 (0.035)	0.729 (0.018)	37.7	10.8	0.998	16
	368 d	−0.020 (0.043)	0.694 (0.022)	44.9	11.0	0.997	16
EPA-13	14 d	0.492 (0.022)	0.742 (0.016)	43.7	13.5	0.999	28
$f_{oc} = 4.50 \times 10^{-2}$	28 d	0.672 (0.039)	0.675 (0.023)	61.9	13.9	0.995	24
	42 d	0.695 (0.062)	0.666 (0.035)	64.3	13.8	0.992	14
EPA-9 Loess	14 d	−1.602 (0.044)	0.848 (0.026)	17.8	8.9	0.998	16
$f_{oc} = 0.12 \times 10^{-2}$	28 d	−1.475 (0.059)	0.810 (0.029)	22.4	9.3	0.996	15
	42 d	−1.456 (0.060)	0.819 (0.030)	23.8	10.3	0.995	16
EPA-8 sediment	14 d	−1.001 (0.092)	0.780 (0.053)	46.7	16.9	0.989	15
$f_{oc} = 0.16 \times 10^{-2}$	28 d	−1.077 (0.066)	0.814 (0.032)	41.4	17.5	0.995	14
	42 d	−1.088 (0.066)	0.843 (0.038)	39.6	16.0	0.993	16
Lachine shale	1 d	1.529 (0.083)	0.691 (0.037)	249	60	0.991	16
$f_{oc} = 8.27 \times 10^{-2}$	2 d	1.714 (0.082)	0.666 (0.038)	366	79	0.990	16
	4 d	1.836 (0.049)	0.658 (0.028)	478	99	0.995	16
	7 d	1.868 (0.083)	0.672 (0.040)	526	116	0.989	16
	11 d	2.014 (0.067)	0.636 (0.033)	695	130	0.992	16
	14 d	2.069 (0.040)	0.617 (0.020)	765	131	0.997	16
	21 d	2.237 (0.042)	0.577 (0.021)	1056	151	0.996	16
	28 d	2.367 (0.028)	0.529 (0.012)	1319	151	0.998	22
	90 d	2.537 (0.017)	0.498 (0.009)	1856	184	0.996	16
	182 d	2.652 (0.029)	0.472 (0.015)	2320	204	0.997	16
	368 d	2.722 (0.037)	0.447 (0.020)	2618	205	0.994	16
Lachine shale kerogen	2 d	2.998 (0.040)	0.610 (0.035)	995	165	0.990	16
$f_{oc} = 53.4 \times 10^{-2}$	7 d	3.241 (0.060)	0.576 (0.028)	1649	234	0.993	16
	14 d	3.248 (0.038)	0.588 (0.019)	1708	256	0.997	16
	28 d	3.419 (0.032)	0.539 (0.014)	2340	280	0.997	22
	90 d	3.676 (0.010)	0.469 (0.007)	3778	328	0.997	16
	182 d	3.653 (0.038)	0.501 (0.023)	3773	379	0.993	16
	368 d	3.762 (0.027)	0.442 (0.017)	4410	338	0.996	16
Norwood shale	2 d	1.763 (0.048)	0.660 (0.021)	177	37	0.997	16
$f_{oc} = 18.94 \times 10^{-2}$	7 d	2.186 (0.043)	0.561 (0.021)	400	53	0.996	16
	14 d	2.216 (0.055)	0.549 (0.029)	420	53	0.992	16
	28 d	2.319 (0.037)	0.577 (0.017)	557	79	0.996	16
	90 d	2.627 (0.014)	0.561 (0.008)	1103	146	0.997	16
	182 d	2.982 (0.040)	0.539 (0.024)	2412	289	0.994	16
	368 d	3.105 (0.037)	0.517 (0.024)	3090	334	0.993	16
Norwood shale kerogen	2 d	3.043 (0.024)	0.538 (0.021)	802	96	0.995	16
$f_{oc} = 65.45 \times 10^{-2}$	7 d	3.340 (0.055)	0.486 (0.026)	1462	137	0.992	16
	14 d	3.549 (0.035)	0.408 (0.018)	2086	137	0.994	16
	28 d	3.525 (0.025)	0.452 (0.011)	2119	170	0.997	22

TABLE 1 (Continued)

sorbent	t	log $K_F(t)$[b]	$n(t)$	$K^*_{oc}(t)$[c] $C^*(t) = 5\ \mu$g/L	$K^*_{oc}(t)$[c] $C^*(t) = 500\ \mu$g/L	R^2	N[d]
Norwood shale kerogen	90 d	3.808 (0.014)	0.418 (0.009)	3848	264	0.994	16
$f_{oc} = 65.45 \times 10^{-2}$	182 d	3.816 (0.039)	0.443 (0.025)	4081	314	0.990	16
	368 d	3.950 (0.024)	0.389 (0.015)	5094	306	0.996	16
Paxton shale	2 d	1.269 (0.090)	0.836 (0.041)	351	165	0.993	16
$f_{oc} = 4.07 \times 10^{-2}$	7 d	1.819 (0.049)	0.649 (0.023)	921	183	0.996	16
	14 d	1.820 (0.059)	0.630 (0.029)	895	163	0.994	16
	28 d	1.754 (0.049)	0.669 (0.023)	819	178	0.995	22
	90 d	2.038 (0.018)	0.561 (0.009)	1323	175	0.996	16
	182 d	2.003 (0.028)	0.582 (0.015)	1263	184	0.998	16
	368 d	2.058 (0.027)	0.546 (0.014)	1352	167	0.998	16
Paxton shale kerogen	2 d	2.662 (0.099)	0.637 (0.044)	729	137	0.987	16
$f_{oc} = 35.1 \times 10^{-2}$	7 d	2.888 (0.068)	0.650 (0.032)	1253	250	0.993	16
	14 d	2.994 (0.057)	0.601 (0.028)	1478	235	0.993	16
	28 d	3.010 (0.037)	0.619 (0.016)	1579	273	0.997	22
	90 d	3.377 (0.018)	0.546 (0.009)	3269	404	0.996	16
	182 d	3.348 (0.047)	0.576 (0.025)	3209	455	0.994	16

[a] Short-term (<14 d) PDR parameters for EPA-22 and 23 and 14 d-sorption isotherm parameters for EPA-8, 9, 13, 20, and 26 were reported in refs 6 and 20, respectively. [b] Units of $K_F(t) = (\mu g/g)/(\mu g/L)^n$. [c] Units of $K^*_{oc}(t) =$ L/g-OC. [d] Number of observations. [e] ( ) = 95% CL of log$K_F(t)$. [f] ( ) = 95% CL of $n(t)$.

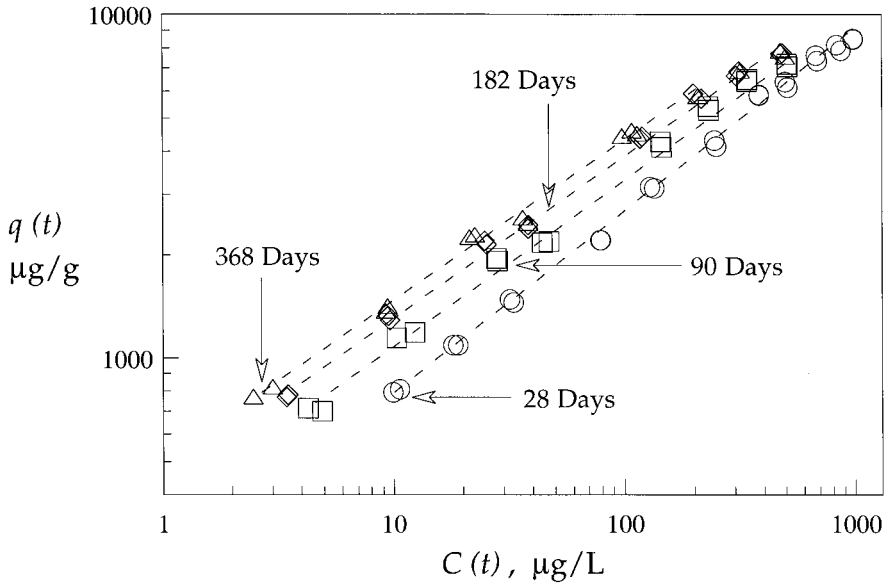

FIGURE 1. Phase distribution relationships measured for Lachine shale at time periods of 28, 90, 182, and 368 days.

yields an arbitrary index value of $K^*_{oc}(t)$ for a specific set of $q(t)$ and $C^*(t)$ values for a soil having a specific f_{oc}:

$$\frac{q(t)}{C^*(t)f_{oc}} = K^*_{oc}(t) \quad (3)$$

It is important to note that $K^*_{oc}(t)$ is not an experimentally determined variable, nor is it a continuous function of either $K_F(t)$ or $n(t)$; its calculated value relates to $K_F(t)$ and $n(t)$ only through the use of these parameters to calculate a value of $q(t)$ for an arbitrary index concentration $C^*(t)$.

Specifically, the calculation was done by computing $q(t)$ values corresponding to two $C^*(t)$ values, 5 and 500 μg/L, from the respective best-fit time-dependent PDR parameters (Table 1). These $q(t)$ and $C^*(t)$ values were then factored into the $K^*_{oc}(t)$ relationship given in eq 3. The $K^*_{oc}(t)$ values for all the samples are presented in Table 1, and those for the $K^*_{oc}(t)$ values for EPA-23 and Lachine shale at $C^*(t)$ of 5 and 500 μg/L are plotted as functions of log t in Figures 3 and 4, respectively. The 95% confidence limits on the calculated $K^*_{oc}(t)$ values are reasonably tight, reflecting those on K_F and n. For example, taking account of the covariance between K_F and n and neglecting variance in f_{oc}, the confidence intervals on the 90 day values of $K^*_{oc}(t) = 64.2$ and 14.7 L/g-OC for the EPA-23 sample at $C^*(t)$ values of 5 and 500 μg/L are 55.6−74.0 L/g-OC and 14.1−15.3 L/g-OC, respectively. Those for Lachine shale values of 1856 and 184 L/g-OC at 90 days are 1754−1959 and 175−192 L/g-OC, respectively.

Temporal PDRs for Shale and Kerogen Samples. Temporal PDRs measured for all shale and kerogen samples were found to become increasingly nonlinear as sorption increased over time. This accords with our previous findings for soils and sediments (*6*). As shown in Figure 2, the nonlinearity (indicated by $n(t)$) of the PDR measured for the Lachine shale sample increases as a function of observation time and corresponding increases in the $K_F(t)$ value. Close inspection of this figure reveals initiation stages ($t \leq 7$ days) and logarithmic stages for both $n(t)$ and $K_F(t)$, patterns similar to those reported earlier (*6*) for several soils and sediments; the latter samples, however, were found to exhibit substantially shorter initiation stages ($t < 30$ min). In the logarithmic stage, $n(t)$ values decrease and $K_F(t)$ values increase as functions of log t. Contrary to the soil and sediment PDR parameters reported earlier, no apparent equilibrium stages

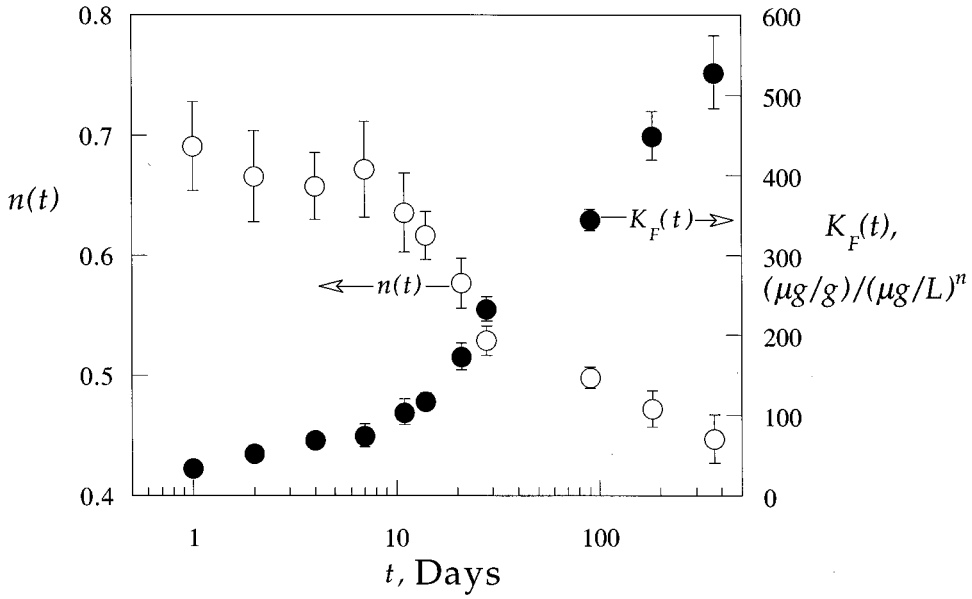

FIGURE 2. Changes of PDR coefficients for sorption of phenanthene by Lachine shale as a function of log time. Error bars represent 95% confidence limits (CL).

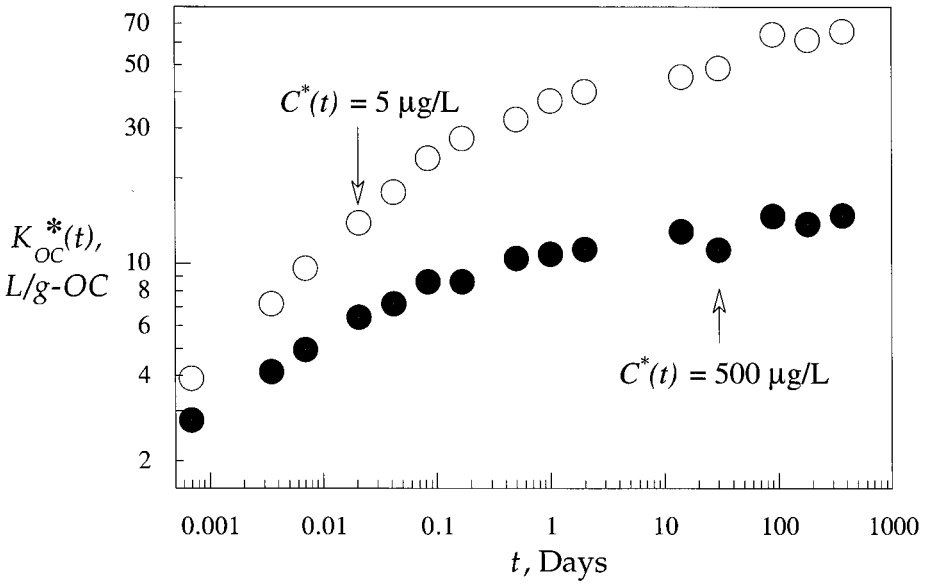

FIGURE 3. Changes in $K^*_{oc}(t)$ value as a function of t for EPA-23 calculated at $C^*(t)$ = 5 and 500 μg/L.

are evident for either $n(t)$ or $K_F(t)$ over the 368 days period of observation, indicating no apparent sorption equilibrium for the Lachine shale over this period. As evidenced in Table 1, the PDR parameters measured for the Lachine kerogen exhibit similar patterns of change; i.e., an initiation stage followed by a logarithmic stage. However, an apparent equilibrium stage appears to exist for both parameters at $t \geq 90$ days, suggesting that sorption by the isolated kerogen sample is relatively faster than that by the parent shale. This could relate to the more ready access of the sorbate to the concentrated form of the kerogen in its extracted state than in its dispersed state in the inorganic matrixes of the parent shale. The other two parent shales and their associated kerogen samples exhibit somewhat different patterns of PDR parameter changes as functions of t. For example, (i) no apparent initiation stage was observed for any of these four systems, likely due to the limited number of measurements made during the initial periods of time, and (ii) apparent equilibrium stages were observed, at least for the Paxton shale and its associated kerogen.

$K^*_{oc}(t)$ Variability. The results given in Table 1 and in Figures 3 and 4 demonstrate that $K^*_{oc}(t)$ ratios for phenanthrene change substantially as a function of aqueous-phase solute concentration for a given sorbent and vary by more than an order of magnitude from sorbent to sorbent. For example, the $C^*(t) = 5$-μg/L $K^*_{oc}(t)$ values at 368 days for EPA-23, Paxton shale, and Norwood kerogen are 65.6, 1352, and 5094 L/g-OC, respectively, whereas the corresponding $C^*(t) = 500$-μg/L $K^*_{oc}(t)$ values at 368 days are 14.8, 167, and 306 L/g-OC. Among these $K^*_{oc}(t)$ values, only the ones obtained at 368 days ~500 μg/L for the seven EPA samples are comparable to the values (8−14 L/g-OC) predicted for phenanthrene using empirical log K_{OC} − log K_{OW}(octanol−water partitioning coefficient) or log K_{OC} − log C_S(solubility) correlations. The large observed variations in $K^*_{oc}(t)$ values among different sorbents is generally in agreement with the observations reported in previous papers in this DRM series (*6*, *27*), but here we note that the absolute values of $K^*_{oc}(t)$ are greatest for these systems that exhibit slow uptake over

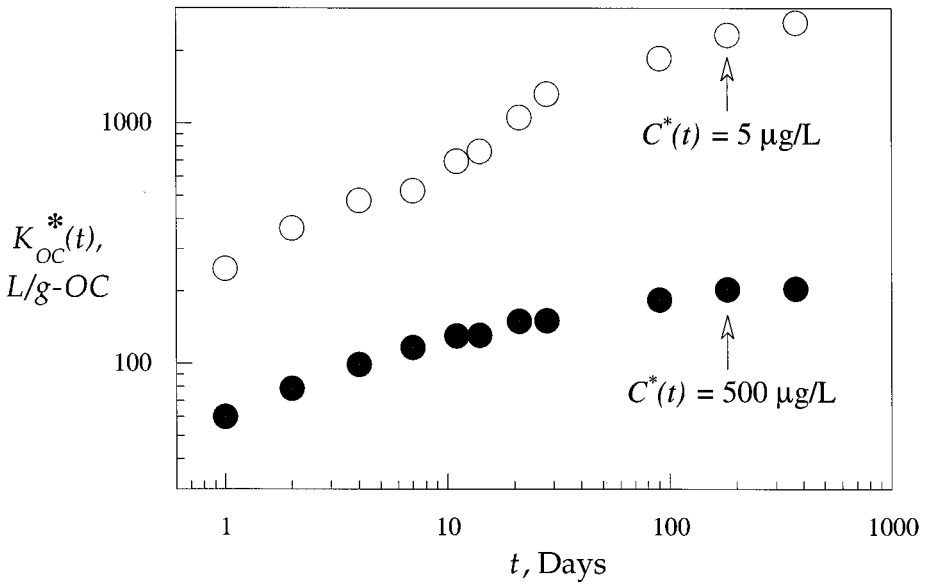

FIGURE 4. Changes in the $K^*_{oc}(t)$ value as a function of t for Lachine shale calculated at $C^*(t) = 5$ and 500 μg/L.

extended time periods. This supports the hypothesis that the more strongly sorbing characteristics of the more condensed and more aromatic organic matter found in our earlier work on sorption equilibria translate into correspondingly slower approaches to equilibrium, presumably because of slower sorbate diffusion through the condensed organic matrixes.

Rate Dependence on Aqueous-Phase Solute Concentration and SOM Type. As indicated earlier, we have defined arbitrary normalizing values of $C^*(t) = 5\,\mu$g/L and $C^*(t) = 500$ μg/L to facilitate comparisons of rates of approach to apparent equilibrium under low and high conditions of solution phase concentration, respectively. This enables calculation of corresponding single-point $K^*_{oc}(t)$ values from eq 3 using $q(t)$ values calculated from the raw data and eq 1. It is evident from the results given in Table 1 and Figures 1−4 that times required for attainment of apparent sorption equilibrium range from hours to more than one year, depending on both aqueous-phase solute concentration, $C(t)$, and the type of geosorbent involved; for example, at an index concentration $C^*(t) = 500$ μg/L, the time required for sorption by EPA-22 and -23 sediment samples to attain relatively constant values of $K^*_{oc}(t)$ is a matter of a few hours, whereas the time is approximately 90 days for the same systems at $C^*(t) = 5$ μg/L. The dependence of rate of sorption on $C^*(t)$ appears to be significant also for EPA-13, EPA-20, and perhaps EPA-9, but it is not apparent for EPA-26 and EPA-8 soil/sediment based on the limited data shown in Table 1. Sorption by the latter samples appears to have attained apparent equilibrium within 14 days at both low ($C^*(t) = 5$ μg/L) and high ($C^*(t) = 500$ μg/L) indexed aqueous phase concentrations.

Kerogens and shales consisting of diagenetically altered SOM exhibit sorption rate phenomena that are markedly different from those for soils and sediments having geologically younger SOM. It has been generally observed in this study that (i) rates of sorption by the kerogen-containing samples are slower than those by the seven humus-containing EPA soil/sediment samples and (ii) the dependence of sorption rate on $C^*(t)$ is more significant for the kerogen-containing samples than for the humus-containing samples. According to Table 1, the time required for attainment of apparent sorption equilibrium at $C^*(t) = 500$ μg/L is about 182 days for all shale and kerogen samples except the Paxton shale, which exhibits a relatively faster rate of sorption. At $C^*(t) = 5$ μg/L, sorption may or may not attain apparent equilibrium within 368 days for at least four (Lachine shale and kerogen and Norwood shale and kerogen) samples, as indicated by substantial increases in $K^*_{oc}(t)$ values for these samples over the period from $t = 182$ to 368 days. In addition, Lachine and Norwood shale samples exhibit relatively slower rates of sorption than their respective kerogen samples. This, along with their relatively smaller $K^*_{oc}(t)$ values, suggests that inorganic matrixes likely act to retard rates of sorption by shale samples, as suggested earlier in this paper.

Significant differences in apparent sorption rates under different $C(t)$ conditions for given sorbate-sorbent systems and among different sorbents having different types of SOM inevitably cause biased rate determinations if measurements of experimental data are initiated at a single $C(t)$ level. For example, Karickhoff et al. (*32*) and Means et al. (*33, 34*) reported that sorptions of polynuclear aromatic hydrocarbons (PAHs)—including phenanthrene—by EPA soils and sediments (including those used in this study) attain equilibrium within a day. The studies on which these reports are based were conducted in CMBR systems at final aqueous-phase solute concentrations equal to about one-tenth the aqueous solubility limit, C_s, of the solutes. Karickhoff (*1*) noted in a later study of the same systems that sorption may not have attained equilibrium even over a period of 5 days. We reported in the fourth paper of this series (*6*) that sorption of phenanthrene by five EPA soils and sediments required about 14 days to attain apparent equilibrium. As noted above, time periods ranging from days to weeks or months have been reported for a variety of sorbent-sorbate systems (*8*). The differences in the reported rates are likely due in part to differences in initial $C(t)$ levels employed and in the types of SOMs the sorbents contained. The sizes of sorbent particles and the physicochemical properties of sorbates may have introduced equally important effects (*4*).

Mechanistic Implications. Considerable evidence has now been obtained to support the argument that SOM consists of at least two major domains: a highly swollen amorphous domain and a relatively condensed rigid domain. The respective behaviors hypothesized for these two domains with respect to isotherm nonlinearity, sorption−desorption hysteresis, and competitive solute interactions have been tested or verified in a number of previous studies (*6, 8, 9, 14, 21−31, 35*). The experimental results of this study provide further support for the argument that diffusion of solute into condensed SOM matrices likely controls the overall rate of

sorption by soils and sediments. The fact that rates of uptake are faster at higher $C(t)$ values appear to relate to the deformation or reconfiguration of condensed SOM matrixes due to solute sorption. In the eighth paper of this series, LeBoeuf and Weber (*9*) found that a purified humic acid transits from a glassy state to a rubbery state upon heating, confirming the existence of two distinctly different SOM domains. It is likely that SOM is a mixture of natural macromolecules having a spectrum of different glass transition temperatures, T_g, the temperature at which polymers transit from their glassy states to rubbery states. Under typical conditions, some fractions of an SOM mixture will have T_g values lower than ambient temperature and some fractions T_g values higher than ambient, thus comprising a composite of swollen and amorphous SOMs and hard and condensed SOMs.

It is known that there are three different types of rate phenomena associated with sorption into glassy polymers, depending upon the way in which the relaxation or reconfiguration of a polymer structure takes place to accommodate sorbing molecules (*14*, *36*, *37*). Case I (Fickian) diffusion occurs if the relaxation rate is much faster than the rate of mass transfer or diffusion of sorbate from the bulk solution phase to a sorption "site", whereas case II (Fickian) diffusion applies when the rate of mass transfer is extremely fast. Case III non-Fickian diffusion occurs if the rates of both solute mass transfer and sorbent relaxation are comparable. Under both case II and case III diffusion conditions, rates of polymer structure relaxation due to uptake of solute molecules are dependent upon the solute concentration within the polymer phase; i.e., the higher $q(t)$ (i.e., higher $C(t)$), the greater is the relaxation of the polymer structure, and the faster is the apparent sorption (i.e., diffusion) rate.

It is likely that local regions of SOM macromolecules existing in their glassy states are reconfigured by phenanthrene penetration and thus become rubbery because their glass transition temperatures are not far above ambient temperatures, as shown by LeBoeuf and Weber (*9*). As the solid-phase solute concentration increases, an increasing fraction of glassy SOM macromolecules become amorphous, and the overall apparent rate of sorption by a soil or sediment increases accordingly.

Acknowledgments

We thank Hong Yu, Zhi Dang, and Henry Harris for their assistance in the experimental phases of the work, and three anonymous reviewers for their comments and suggestions. This research was funded in part by the U.S. Environmental Protection Agency, Office of Research and Development and Grant R-819605 to the Great Lakes and Mid-Atlantic Center (GLMAC) for Hazardous Substance Research. Partial funding of the research activities of GLMAC is also provided by the State of Michigan Department of Environmental Quality.

Literature Cited

(1) Karickhoff, S. W. In *Contaminants and Sediments: Analysis, Chemistry, and Biology*; Baker, R. A., Ed.; Ann Arbor Science; Ann Arbor, MI, 1980; Vol. 2, pp 193−205.
(2) Miller, C. T.; Weber, W. J., Jr. *J. Contam. Hydrol.* **1986**, *1*, 243−261.
(3) Weber, W. J., Jr.; Miller, C. T. *Water Res.* **1988**, *22*, 457−464.
(4) Ball, W. P.; Roberts, P. V. *Environ. Sci. Technol.* **1991**, *25*, 1237−1249.
(5) Pedit, J. A.; Miller, C. T. *Environ. Sci. Technol.* **1994**, *28*, 2094−2104.
(6) Weber, W. J., Jr.; Huang, H. *Environ. Sci. Technol.* **1996**, *30*, 881−888.
(7) Alexander, M. *Environ. Sci. Technol.* **1995**, *29*, 2713−2717.
(8) Pignatello, J. J.; Xing, B. *Environ. Sci. Technol.* **1996**, *30*, 1−11.
(9) LeBoeuf, E. J.; Weber, W. J., Jr. *Environ. Sci. Technol.* **1997**, *31*, 1697−1702.
(10) Pignatello, J. J. In *Reactions and Movements of Organic Chemicals in Soils*; Sawhney, B. L., Brown, K., Eds.; Soil Science Society of America: Madison, WI, 1989; Chapter 3.
(11) Curtis, G. P.; Reinhard, M.; Roberts, P. V. In *Geochemical Processes at Mineral Surfaces*; Davis, J. A., Hayes, K. F., Eds.; American Chemical Society: Washington D.C.
(12) Ball, W. P. *Equilibrium Sorption and Diffusion Rate Studies with Halogenated Organic Chemical and Sandy Aquifer Material*; Ph.D. Dissertation, Stanford University, Stanford, CA, 1990.
(13) Brusseau, M. L.; Jessup, R. E.; Rao. P. S. *Environ. Sci. Technol.* **1991**, *25*, 134−142.
(14) LeBoeuf, E. J. *Macromolecular Characteristics of Natural Organic Matter and Their Influence on Sorption and Desorption Behavior of Organic Chemicals*; Ph.D. Dissertation, The University of Michigan, Ann Arbor, MI, 1998.
(15) Wu, S.; Gschwend, P. M. *Environ. Sci. Technol.* **1986**, *20*, 717−725.
(16) Farrell, J.; Reinhard, M. *Environ. Sci. Technol.* **1994**, *28*, 63−72.
(17) Werth, C. J.; Reinhard, M. *Environ. Sci. Technol.* **1997**, *31*, 697−703.
(18) Crittenden, J. C.; Hutzler, N. J.; Geyer, D. G.; Oravitz, J. L.; Friedman, G. *Water Res. Resear.* 1986, *22*, 271−284.
(19) Connaughton, D. F.; Stedinger, J. R.; Lion, L. W.; Shuler, M. L. *Environ. Sci. Technol.* **1993**, *27*, 2397−2403.
(20) Holmen, B. A.; Gschwend P. M. *Environ. Sci. Technol.* **1997**, *31*, 105−113.
(21) Huang, W.; Schlautman, M. A.; Weber, W. J., Jr. *Environ. Sci. Technol.* **1996**, *30*, 2993−3000.
(22) Weber, W. J., Jr.; McGinley, P. M.; Katz, L. E. *Environ. Sci. Technol.* **1992**, *26*, 1955−1962.
(23) McGinley, P. M.; Katz, L. E.; Weber, W. J., Jr. *Environ. Sci. Technol.* **1993**, *27*, 1524−1531.
(24) Young, T. M.; Weber, W. J., Jr. *Environ. Sci. Technol.* **1995**, *29*, 92−97.
(25) Weber, W. J., Jr.; Young, T. M. *Environ. Sci. Technol.* **1997**, *31*, 1686−1691.
(26) Young, T. M.; Weber, W. J., Jr. *Environ. Sci. Technol.* **1997**, *31*, 1692−1696.
(27) Huang, W.; Young, T. M.; Schlautman, M. A.; Yu, H.; Weber, W. J., Jr. *Environ. Sci. Technol.* **1997**, *31*, 1703−1710.
(28) Huang, W.; Weber, W. J., Jr. *Environ. Sci. Technol.* **1997**, *31*, 2562−2569.
(29) Xing, B.; Pignatello, J. J.; Gigliotti, B. *Environ. Sci. Technol.* **1996**, *30*, 2432−2440.
(30) Xing, B.; Pignatello, J. J. *Environ. Sci. Technol.* **1997**, *31*, 792−799.
(31) Huang, W.; Yu, H.; Weber, W. J., Jr. *J. Contaminant Hydrol.* **1998**, *31*, 129−148.
(32) Karickhoff, S. W.; Brown, D. S.; Scott, T. A. *Water Res.* **1979**, *13*, 241−248.
(33) Means, J. C.; Wood, S. G.; Hassett, J. J.; Banwart, W. L. *Environ. Sci. Technol.* **1980**, *14*, 1524−1528.
(34) Means, J. C.; Wood, S. G.; Hassett, J. J.; Banwart, W. L. *Environ. Sci. Technol.* **1982**, *16*, 93−98.
(35) Carroll, K. M.; Harkness, M. R.; Bracco, A. A.; Balcarcel, R. R. *Environ. Sci. Technol.* **1994**, *28*, 253−258.
(36) Crank, J. *The Mathematics of Diffusion*, 2nd ed.; Oxford University Press: Oxford, U.K., 1975.
(37) Crank, J.; Park, G. S. *Diffusion in Polymers*; Academic Press: London and New York, 1968.

Received for review August 27, 1997. Revised manuscript received August 6, 1998. Accepted August 26, 1998.

ES970764N